AN ELECTRON DENSITY MODEL FOR SATURN'S INNER MAGNETOSPHERE

A. M. Persoon*, D. A. Gurnett*, W. S. Kurth*,
G. B. Hospodarsky*, J. B. Groene*,
P. Canu†, and M. K. Dougherty‡

Abstract

Electron density profiles have been derived from near-continuous upper hybrid resonance emissions, obtained by the Radio and Plasma Wave Science (RPWS) instrument on the Cassini spacecraft for three equatorial orbits of Saturn during February and March, 2005. Independent verification of the upper hybrid frequency has also been obtained from the RPWS sounder. The upper hybrid frequency and the electron cyclotron frequency, derived from the magnetic field measurements of the magnetometer instrument, are used to determine the electron densities with a high degree of accuracy, providing near-continuous electron density profiles for Saturn's magnetosphere inside 9 saturnian radii (R_S). Electron density profiles for these orbits are consistently repeatable, decreasing with increasing radial distance outside 5 R_S. The radial dependence is consistent with an outward radial expansion of the plasma beyond 5 R_S. Inside 5 R_S, the profiles show a high degree of variability from orbit to orbit, even between the inbound and outbound portions of the same orbit, suggesting that the source of the radial expansion of the plasma lies in this region. Possible plasma sources in this region, which include the moons Enceladus and Tethys and the E ring, are expected to contribute to the variations in the density profiles.

1 Introduction

The Cassini spacecraft is the most recent spacecraft to obtain plasma measurements of Saturn's inner magnetosphere. The first in situ measurements were made by the plasma instruments on Pioneer 11 and on Voyagers 1 and 2 during their flybys of the planet in 1979, 1980 and 1981 [Bridge et al., 1981, 1982; Frank et al., 1980; Sittler et al., 1983]. From these early measurements, models were derived to explain the observed

* *Dept. of Physics and Astronomy, University of Iowa, Iowa City, IA 52242, USA*
† *CETP-UVSQ/IPSL, 10-12 avenue de l'Europe, Velizy, France*
‡ *The Blackett Laboratory, Imperial College, London, UK*

plasma composition and distribution [Richardson and Sittler, 1990; Richardson, 1995, 1998]. More recent plasma measurements have been made with the arrival of Cassini at Saturn on July 1, 2004 [Gurnett et al., 2005; Young et al., 2005]. The Cassini spacecraft, which carries several instruments capable of measuring the plasma density, has made it possible to expand on earlier plasma density models. The Radio and Plasma Wave Science (RPWS) instrument [Gurnett et al., 2004] on Cassini has consistently observed narrowband upper hybrid resonance emissions below 100 kHz inside of $\sim$10 R_S [Gurnett et al., 2005]. The electron density profiles, derived from the Cassini measurements of the upper hybrid frequency, are, in some respects, comparable to the density profiles derived from the Pioneer 11 and Voyagers 1 and 2 measurements. Cassini is scheduled to make 76 orbits of Saturn during its prime mission, making it possible for the first time to obtain density measurements over multiple consecutive orbits of Saturn and to investigate the radial and latitudinal dependences of the plasma distribution. The purpose of this paper is to study the radial distribution of the electron densities near the equatorial plane in Saturn's inner magnetosphere.

2 Density Measurement Technique

This study of Saturn's equatorial densities employs the well-established technique of using the upper hybrid resonance frequency to determine the electron density [Mosier et al., 1973; Warwick et al., 1979; Gurnett et al., 1981]. A narrow band of electrostatic emissions centered on the upper hybrid resonance frequency, labeled f_{UHR}, is clearly visible just below 100 kHz in Fig. 1. This frequency-time spectrogram is from Cassini's pass through Saturn's inner magnetosphere beginning at 22:00 Universal Time (UT) on March 8, 2005 and ending at 00:00 UT on March 10, 2005. During this time the spacecraft moved inward toward Saturn from a radial distance of 9.23 R_S at the beginning of the plot, through periapsis at 3.56 R_S at 11:40 UT and outward to 8.6 R_S at the end of the plot. Throughout this time interval, Cassini remained very close to the equatorial plane, with a maximum latitude of 0.21 degrees.

For this pass, the nearly continuous upper hybrid resonance emission band shows a high degree of symmetry with respect to periapsis. The upper hybrid resonance frequency steadily increases with decreasing radial distance, from 28 kHz at 8.4 R_S at 23:40 UT to a maximum frequency of 78 kHz at 4.7 R_S at 07:11 UT on the inbound pass. On the outbound pass, the upper hybrid resonance frequency decreases with increasing radial distance from a maximum frequency of 72 kHz at 4.8 R_S at 16:15 UT to 26 kHz at 8.1 R_S at 22:54 UT on March 9. Inside of 4.7 R_S, the upper hybrid resonance frequency drops to a broad minimum frequency of $\sim$57 kHz from 10:15 UT until 12:45 UT. On both the inbound and outbound passes, the upper hybrid emission line is smooth and continuous inside 6.5 R_S, becomes sporadic and weaker beyond 6.5 R_S, and is undetectable beyond 8.4 R_S. These upper hybrid resonance frequency measurements are used to determine the electron densities in Saturn's inner magnetosphere.

¿From the basic definition of the upper hybrid resonance frequency [Gurnett and Bhattacharjee, 2005], the electron density n_e (cm^{-3}) is derived from the upper hybrid frequency

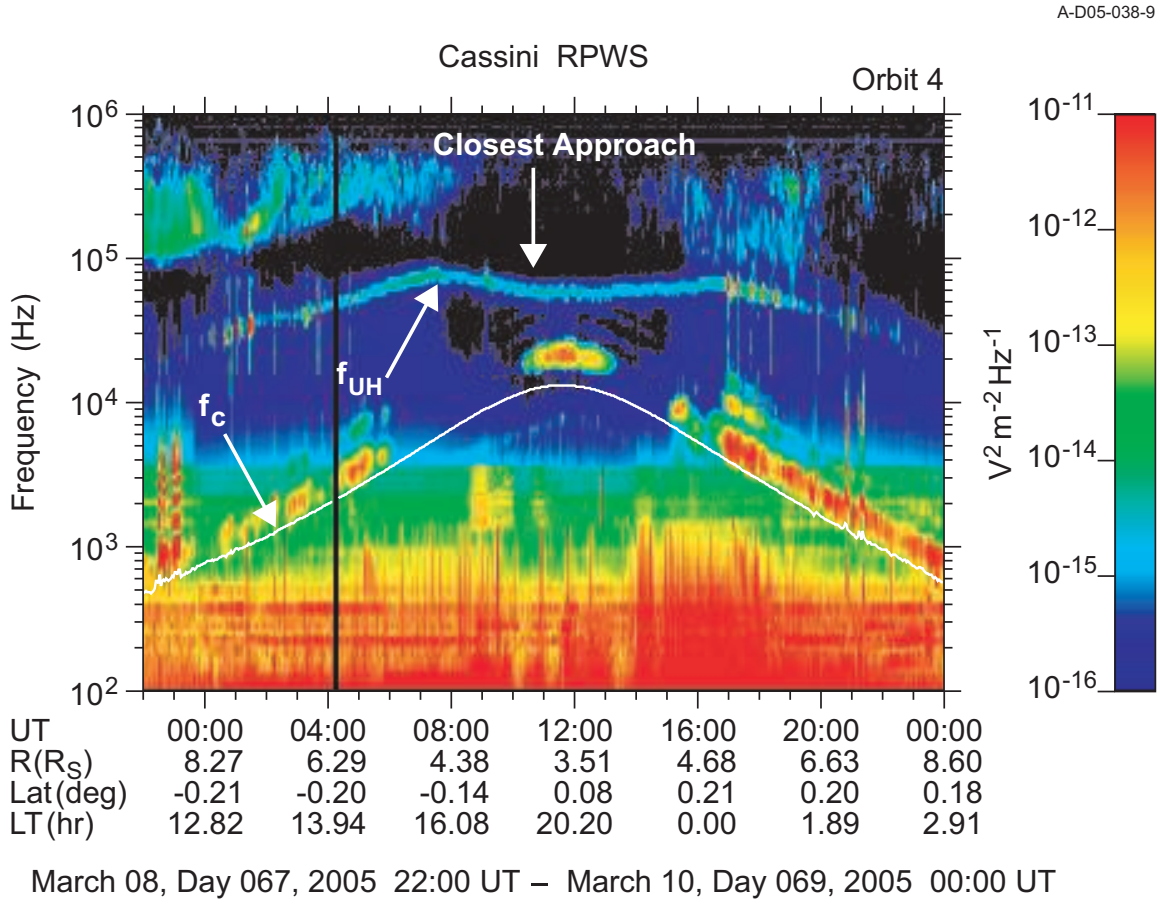

Figure 1: A frequency-time spectrogram showing the electric field intensities detected by the RPWS instrument during Cassini's pass through Saturn's inner magnetosphere on March 8-10, 2005. The narrowband emissions just below 100 kHz are the upper hybrid resonance emissions. The white line below 15 kHz is the electron cyclotron frequency, derived from the magnetometer measurements. Cassini's closest approach to Saturn occurs at 11:40 UT.

f_{UH} (Hz), using

$$n_e = \frac{f_{UH}^2 - f_c^2}{8980^2}, \tag{1}$$

where f_c is the electron cyclotron frequency in Hz. The electron cyclotron frequency, shown as a white line below 15 kHz in Fig. 1, has been derived from the magnetometer measurements of the magnetic field [Dougherty et al., 2004] using $f_c = 28 \times B$ (Hz) where B is the magnitude of the field in nanoteslas.

There are two techniques used by the RPWS to determine the upper hybrid resonance frequency. The active technique uses the RPWS sounder transmitter [Gurnett et al., 2004] to excite electrostatic oscillations at the upper hybrid resonance frequency. The passive technique measures the peak frequency at the center of the narrow band of thermally excited electrostatic emissions that are nearly continuous on Cassini's passes through the inner magnetosphere.

The RPWS High Frequency Receiver samples 288 discrete frequencies between 3.5 kHz and 16 MHz, a frequency range that includes the full range of the upper hybrid resonance frequency measurements. A full sweep of the frequency range is made every 8 seconds. Fig. 2 is an RPWS spectral density plot spanning the frequency range of 10-100 kHz just before closest approach at 10:44:20 UT on March 9, 2005. This portion of the frequency spectrum shows two distinct emissions, the electron cyclotron harmonic emission centered on 21 kHz and the upper hybrid resonance emission band between 48 and 70 kHz. Both appear as solid black lines in the plot. The passive technique identifies the upper hybrid resonance frequency in two steps using automatic data processing algorithms. These two steps are illustrated in Fig. 2. In the first step, a data processing algorithm is used to identify the peak frequency in the f_{UH} emission band. The peak frequency is marked with a black triangle at 57 kHz.

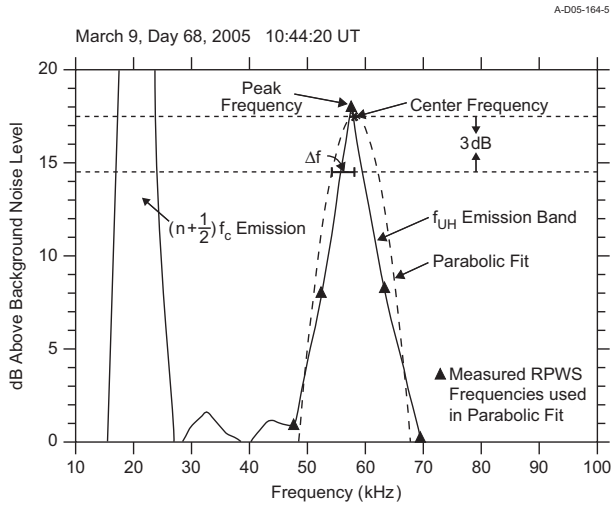

Figure 2: A spectral density plot of wave amplitude vs. frequency for the 10 kHz – 100 kHz portion of the RPWS frequency spectrum on March 9, 2005 at 10:44:20 UT, showing the steps in the data processing algorithm used to identify the upper hybrid resonance frequency and the uncertainty in the frequency determination. The electron density is determined to be 40±5 cm^{-3}.

The second step of the passive technique employs a least squares parabolic fit to the peak frequency and the two frequency measurements on either side (all five frequencies are marked with black triangles in Fig. 2). The parabolic fit (shown as a dashed line) determines a center frequency for the emission band that does not depend on the discrete nature of the frequency sampling by the RPWS. The center frequency, located at 58.2 kHz, is shown by an open circle. Using the above equation, the electron density is determined to be 40 cm^{-3}. The uncertainty in the electron density is related to the width of the emission band by determining the half-width of the parabolic fit at 3 dB below the center frequency. The uncertainty, in kHz, is labeled Δf in Fig. 2. For well-defined, narrow f_{UH} emission bands like the one in Fig. 2, the uncertainty in the density determination is small, $\Delta n_e/n_e \approx 13\%$. This accuracy degrades in regions where the signal to noise ratio is poor, i.e., less than 3 dB. This is especially true at larger radial distances beyond $\sim$6.5 R_S.

The electron density profiles from both the active and passive measurements of the upper hybrid resonance frequency for the time interval shown in Fig. 1 are shown in Fig. 3. The overlap of the two density profiles indicates a good agreement between these independently derived density measurements. There is a high degree of symmetry between the inbound and outbound portions of the density profile. The densities increase with decreasing radial distance to a maximum density of 76 cm^{-3} at 4.7 R_S for the inbound portion of the pass and a maximum density of 63 cm^{-3} at 4.8 R_S for the outbound portion of the pass. Inside 5 R_S, the densities initially decrease with decreasing radial distance on the inbound pass and then increase again after 12:45 UT on the outbound pass, as the spacecraft moves away from the planet. The densities are nearly constant at ∼40 cm^{-3} from 10:15 UT until 12:45 UT.

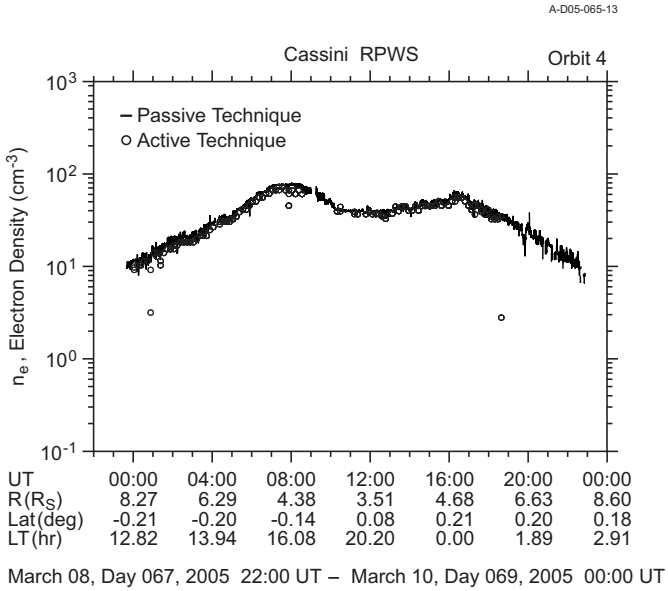

Figure 3: The electron density profiles from both the active (open circles) and passive (solid line) measurements of the upper hybrid resonance frequency for the time interval shown in Fig. 1. The overlap of the two density profiles indicates a good agreement between these independently derived density measurements.

The three very low density values in the sounder data in Fig. 3 are sudden and significant drop-outs in the density profile, believed to be due to flux tube interchange motions where plasma in low-density flux tubes moves inward, replacing plasma in the centrifugally-driven, high-density magnetic flux tubes and transporting mass outward [Andre et al., 2005; Burch et al., 2005; Hill et al., 2005]. Similar density depletions have not been included in the density profiles derived from the passive technique. Densities derived using the passive technique cannot be determined with the same degree of certainty inside these density-depleted flux tubes as they can outside the flux tubes because of broadening of the upper hybrid emission band due to hot plasma effects. These density drop-outs represent less than 1% of the total density measurements derived using the passive technique.

3 Equatorial Electron Densities

In February and March 2005, Cassini passed through Saturn's inner magnetosphere very close to the equatorial plane on three consecutive orbits. Fig. 4 shows the Cassini trajectories for these orbits: February 16-17, 2005 (Orbit 3); March 8–9, 2005 (Orbit 4); and March 29-30, 2005 (Orbit 5). We have selected these three orbits because Cassini remained within ± 0.1 R_S of Saturn's equatorial plane for radial distances inside 10 R_S. The fact that these orbits are so tightly constrained in latitude makes it possible to study the equatorial radial dependence of the electron population without considering latitudinal variations. With the exception of several large data gaps on the inbound portion of orbit 5, the f_{UHR} emission bands are nearly continuous throughout the inner magnetosphere. For all three orbits, Cassini's closest approach to Saturn is 3.5 R_S.

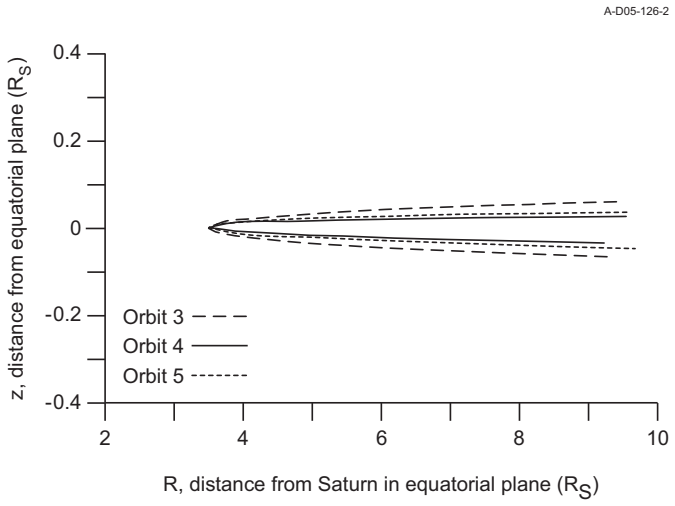

Figure 4: A composite plot of the Cassini trajectories for three consecutive equatorial orbits: February 16-17, 2005 (Orbit 3); March 8-9, 2005 (Orbit 4); and March 29-30, 2005 (Orbit 5). Spacecraft position projected on the equatorial plane is given in saturnian radii on the horizontal axis and its position above/below the equatorial plane is given in saturnian radii on the vertical axis. The spacecraft remained within ± 0.1 R_S of Saturn's equatorial plane for radial distances inside 10 R_S. Cassini's closest approach to Saturn is 3.5 R_S.

The electron density profiles for these three equatorial orbits are shown in Fig. 5. Since the passive spectrum measurements have a better time resolution (one measurement every 8 seconds in the inner magnetosphere) than the sounder measurements (two consecutive measurements every 10 minutes), only the passive measurements are shown in this plot. The densities for the inbound and outbound portions of each orbit are plotted as a function of radial distance. On orbits 3 and 4, the longitudinal differences between the orbits vary by less than 20°, from 62° (orbit 3) and 46° (orbit 4) on the inbound passes to 238° (orbit 3) and 257° (orbit 4) on the outbound passes. The longitudes for orbit 5 range from 204° on the inbound to 349° on the outbound.

The most striking feature of these density profiles is the strong, consistent radial dependence beyond 5 R_S, varying as $(1/R)^{3.2}$ to $(1/R)^{4.1}$. The exception is the incomplete

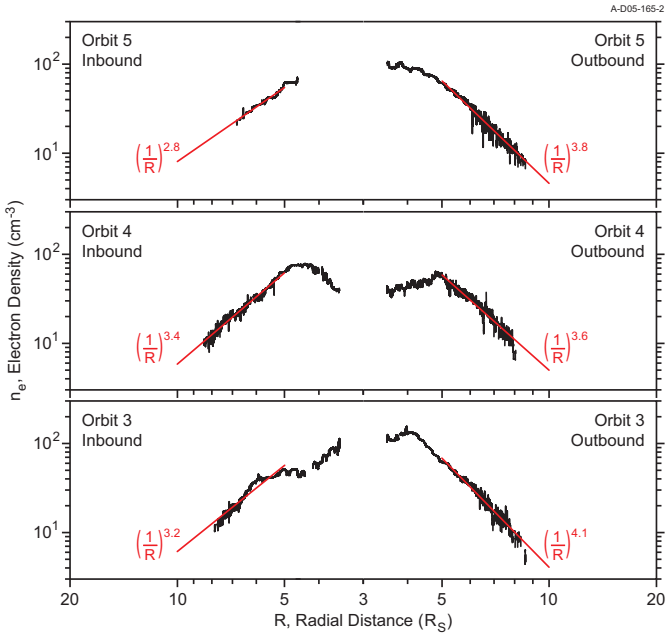

Figure 5: The electron density profiles for three consecutive equatorial orbits as a function of radial distance from the planet, with the inbound portion of the orbits on the left (moving toward the planet) and the outbound portion of the orbits on the right (moving away from the planet). The density profiles exhibit a consistent radial dependence beyond 5 R_S*, varying as* $(1/R)^{3.2}$ *to* $(1/R)^{4.1}$*. The exception is the incomplete density profile for the inbound portion of orbit 5.*

density profile for the inbound portion of orbit 5 where there are several large data gaps. The radial dependence of the plasma distribution beyond 5 R_S for these orbits is consistent with the radial dependence predicted for the equatorial densities in the model derived by Persoon et al. [2005]. Densities at 5 R_S range from 50-63 cm^{-3} on the inbound passes and from 56-62 cm^{-3} on the outbound passes. At 8 R_S, densities range from 12-13 cm^{-3} on the inbound passes and from 10-11 cm^{-3} on the outbound passes. The orbit-to-orbit consistency of the electron density profiles in Fig. 5 beyond 5 R_S strongly suggests that the plasma has reached a steady-state equilibrium and is expanding radially outward.

Both the inverse radial dependence and the measured densities are in good agreement with the plasma density profile derived from the Pioneer 11 flyby measurements for the same radial distance [Frank et al., 1980]. The trajectory of Pioneer 11 remained within 0.5 R_S of the equatorial plane during the Saturn flyby, similar to the trajectories of Cassini for these three equatorial passes. However, the trajectories of the Voyager spacecraft passed through Saturn's inner magnetosphere at much higher latitudes. Voyager 1 spanned a latitude range of -8.5° to 10.2°, reaching a maximum latitude of -41° near closest approach and spending less than 12 minutes within 0.5° of the equatorial plane. Within 10 R_S, Voyager 2 spanned a latitude range of -29° to 22° and spent less than 5 minutes within 0.5° of the equatorial plane. The peak densities observed by Voyagers 1 and 2 [Bridge et al., 1981, 1982] are 50-65% lower than the RPWS measurements, all of which were acquired within 0.4° of the equatorial plane. The lower Voyager densities are to be expected since,

throughout most of the pass through Saturn's inner magnetosphere, the trajectories of the Voyager spacecraft were at much higher latitudes where plasma densities are expected to be lower. Plasma densities will be highest near the equatorial plane, because the dominant centrifugal force acting on the co-rotating plasma will cause the plasma to concentrate along those parts of the magnetic field lines which are farthest from the rotational axis [Gledhill, 1967]. Saturn's magnetic axis is nearly aligned with its rotational axis, so plasma is expected to accumulate near the equatorial plane. Power law radial dependences of L^{-3} and L^{-4}, projected onto the equatorial plane, were inferred from the Voyager density measurements [Bridge et al., 1981, 1982]. The radial dependences of $(1/R)^{3.2}$ to $(1/R)^{4.1}$ in Fig. 5 are consistent with the radial dependences of the Voyager analyses.

Inside 5 R_S, the density profiles in Fig. 5 are highly variable. For orbit 4 (inbound and outbound) and orbit 3 (outbound), the densities show a strong radial dependence, increasing with increasing radial distance. This suggests that there is a plasma source in this region. However, the densities for orbit 3 (inbound) and orbit 5 (outbound) inside 5 R_S continue to decrease with increasing radial distance, although the radial dependence is weaker than it is outside 5 R_S. Also highly variable is the distance where the plasma density distribution changes from the highly variable radial dependence to the consistent, power-law radial dependence characteristic of a steady-state, outward radial expansion of the plasma. For the inbound passes, the transition, indicated by the peak in the density profile, consistently occurs very close to 5 R_S. However, the transition point is more variable for the outbound passes, from 3.8 R_S in orbit 5 to 4.9 R_S in orbit 4.

Local time and longitudinal effects do not appear to provide an explanation for the variability in the density profiles in this region. Inside 5 R_S, Cassini spanned a similar range of local times for all three orbits, from 15.2±0.1 hours on the inbound portion of the orbits to 0.4±0.1 hours on the outbound portion of the orbits, with closest approach at 19.7±0.1 hours. The range of longitudes for orbits 3 and 4 differ by less than 20°, but the differences in the radial dependences between the inbound portions of these two orbits, as well as the location of the peak densities for the outbound portions of the two orbits, are significant. And, although the longitudes for orbits 3 and 5 differ by more than 70°, the locations of the peak densities on the outbound portions of these two orbits are similar. These three equatorial density profiles, however, are not sufficient to rule out the possibility of longitudinal and local time effects on the density distribution in the inner magnetosphere. And other factors, such as variations in the solar wind and the interplanetary magnetic field, would contribute to changes in Saturn's magnetosphere that could subsequently contribute to the shift in the peak densities from orbit to orbit.

The large variability in the density profiles inside 5 R_S and the large differences in the location of the peak densities on the outbound portions of the orbits suggest that the plasma has not achieved equilibrium and that there are likely plasma sources in this region contributing to the spatial and temporal variations in the electron density profiles. Saturn's moon Enceladus is now known to be a significant source of neutral gases and plasma in the form of water group ions [Dougherty et al., 2006; Hansen et al., 2006; Tokar et al., 2006; Waite et al., 2006]. Enceladus and other potential plasma sources, such as the E ring, will undoubtedly influence the global, long-term distribution of plasma in this region.

4 Summary

Electron density profiles, derived from the RPWS measurements of the upper hybrid resonance frequency for three consecutive equatorial Cassini passes through Saturn's inner magnetosphere, show a consistent and repeatable power-law radial dependence beyond 5 R_S, varying from $(1/R)^{3.2}$ to $(1/R)^{4.1}$, consistent with a steady-state outward radial expansion of the plasma. Inside 5 R_S, the density profiles are highly variable from orbit to orbit, even between the inbound and outbound portions of the same orbit. The factors contributing to the variability of the density profiles inside 5 R_S are undoubtedly complex and have not yet been determined.

References

Andre, N., M. K. Dougherty, C. T. Russell, J. S. Leisner, and K. K. Khurana, Dynamics of the Saturnian inner magnetosphere: First inferences from the Cassini magnetometers about small-scale plasma transport in the magnetosphere, *Geophys. Res. Lett.,* **32,** L14S06, 2005.

Bridge, H. S., J. W. Belcher, A. J. Lazarus, S. Olbert, J. D. Sullivan, F. Bagenal, P. R. Gazis, R. E. Hartle, K. W. Ogilvie, J. D. Scudder, E. C. Sittler, A. Evietar, G. L. Siscoe, C. K. Goertz and V. M. Vasyliunas, Plasma observations near Saturn: Initial results from Voyager 1, *Science,* **212,** 217–224, 1981.

Bridge, H. S., F. Bagenal, J. W. Belcher, A. J. Lazarus, R. L. McNutt, J. D. Sullivan, P. R. Gazis, R. E. Hartle, K. W. Ogilvie, J. D. Scudder, E. C. Sittler, A. Evietar, G. L. Siscoe, C. K. Goertz and V. M. Vasyliunas, Plasma observations near Saturn: Initial results from Voyager 2, *Science,* **215,** 563–570, 1982.

Burch, J. L., J. Goldstein, T. W. Hill, D. T. Young, F. J. Crary, A. J. Coates, N. Andre, W. S. Kurth, and E. C. Sittler, Jr., Properties of local plasma injections in Saturn's magnetosphere, *Geophys. Res. Lett.,* **32,** L14S02, 2005.

Dougherty, M. K., S. Kellock, D. J. Southwood, A. Balogh, E. J. Smith, B. T. Tsurutani, B. Gerlach, K.-H. Glassmeier, F. Gleim, C. T. Russell, G. Erdos, F. M. Neubauer and S. W. H. Cowley, The Cassini magnetic field investigation, *Space Sci. Rev.,* **114,** 331–383, 2004.

Dougherty, M. K., K. K. Khurana, F. M. Neubauer, C. T. Russell, J. Saur, J. S. Leisner and M. E. Burton, Identification of a dynamic atmosphere at Enceladus with the Cassini magnetometer, *Science*, **311**, 1406–1409, doi: 10.1126/science.1120985, 2006.

Frank, L. A., B. G. Burek, K. L. Ackerson, J. H. Wolfe and J. D. Mihalov, Plasmas in Saturn"s magnetosphere, *J. Geophys. Res.,* **85,** 5695–5708, 1980.

Gledhill, J. A., Magnetosphere of Jupiter, *Nature,* **214,** 115, 1967.

Gurnett, D. A., W. S. Kurth, and F. L. Scarf, Plasma waves near Saturn: Initial results from Voyager 1, *Science,* **212,** 235–239, 1981.

Gurnett, D. A., W. S. Kurth, D. L. Kirchner, G. B. Hospodarsky, T. F. Averkamp, P. Zarka, A. Lecacheux, R. Manning, A. Roux, P. Canu, N. Cornilleau-Wehrlin, P. Galopeau, A. Meyer, R. Bostrom, G. Gustafsson, J.-E. Wahlund, L. Ahlen, H. O. Rucker, H. P Ladreiter, W. Macher, L.J.C. Wooliscroft, H. Alleyne, M. L. Kaiser, M. D. Desch, W. M. Farrell, C. C. Harvey, P. Louarn, P. J. Kellogg, K. Goetz and A. Pedersen, The Cassini radio and plasma wave investigation, *Space Sci. Rev.,* **114,** 395–463, 2004.

Gurnett, D. A., W. S. Kurth, G. B. Hospodarsky, A. M. Persoon, T. F. Averkamp, B. Cecconi, A. Lecacheux, P. Zarka, P. Canu, N. Cornilleau-Wehrlin, P. Galopeau, A. Roux, C. Harvey, P. Louarn, R. Bostrom, G. Gustafsson, J.-E. Wahlund, M. D. Desch, W. M. Farrell, M. L. Kaiser, K. Goetz, P. J. Kellogg, G. Fischer, H. P Ladreiter, H. Rucker, H. Alleyne and A. Pedersen, Radio and plasma wave observations at Saturn from Cassini"s approach and first orbit, *Science,* **307,** 1255–1259, 2005.

Gurnett, D. A. and A. Bhattacharjee, *Introduction to Plasma Physics with Space and Laboratory Applications,* Cambridge Univ. Press, Cambridge, p. 112, 2005.

Hansen, C.J., L. Esposito, A. I. F. Stewart, J. Colwell, A. Hendrix, W. Pryor, D. Shemansky, and R. West, Enceladus' water vapor plume, *Science*, **311**, 1422-1425, doi: 10.1126/science.1121254, 2006.

Hill, T. W., A. M. Rymer, J. L. Burch, F. J. Crary, D. T. Young, M. F. Thomsen, D. Delapp, N. Andre, A. J. Coates, and G. R. Lewis, Evidence for rotationally driven plasma transport in Saturn's magnetosphere, *Geophys. Res. Lett.,* **32,** L14S10, 2005.

Mosier, S. R., M. L. Kaiser, and L. W. Brown, Observations of noise bands associated with the upper hybrid resonance by the Imp 6 radio astronomy experiment, *J. Geophys. Res.,* **78,** 1673–1679, 1973.

Persoon, A. M., D. A. Gurnett, W. S. Kurth, G. B. Hospodarsky, J. B. Groene, P. Canu, and M. K. Dougherty, Equatorial electron density measurements in Saturn"s inner magnetosphere, *Geophys. Res. Lett.,* **32,** L23105, doi:10.1029/2005GL024294, 2005.

Richardson, J. D. and E. C. Sittler, Jr., A plasma density model for Saturn based on Voyager observations, *J. Geophys. Res.,* **95,** 12,019–12,031, 1990.

Richardson, J. D., An extended plasma model for Saturn, *Geophys. Res. Lett.,* **22,** 1177–1180, 1995.

Richardson, J. D., Thermal plasma and neutral gas in Saturn"s magnetosphere, *Rev. Geophys.,* **36,** 501–524, 1998.

Sittler, E. C., Jr., K. W. Ogilvie, and J. D. Scudder, Survey of low-energy plasma electrons in Saturn"s magnetosphere, *J. Geophys. Res.,* **88,** 8847–8870, 1983.

Tokar, R. L., R. E. Johnson, T. W. Hill, D. H. Pontius, W. S. Kurth, F. J. Crary, D. T. Young, M. F. Thomsen, D. B. Reisenfeld, A. J. Coates, G. R. Lewis, E. C. Sittler, and D. A. Gurnett, The interaction of the atmosphere of Enceladus with Saturn's plasma, *Science*, **311**, 1409–1412, doi: 10.1126/science.1121061, 2006.

Waite, J. H., Jr., M. Combi, W.-H. Ip, T. E. Cravens, R. L. McNutt, Jr., W. Kasprzak, R. Yelle, J. Luhmann, H. Niemann, D. Gell, B. Magee, G. Fletcher, J. Lunine and W.-L. Tseng, The atmospheric plume of Enceladus as observed by the Cassini ion neutral mass spectrometer, *Science*, **311**, 1419–1422, doi: 10.1126/science.1121290, 2006.

Warwick, J. W., J. B. Pearce, A. C. Riddle, J. K. Alexander, M. D. Desch, M. L. Kaiser, J. R. Thieman, T. D. Carr, S. Gulkis, A. Boischot, C. C. Harvey, and B. M. Pedersen, Voyager 1 planetary radio astronomy observations near Jupiter, *Science,* **204,** 995–998, 1979.

Young, D. T., J.-J. Berthelier, M. Blanc, J. L. Burch, S. Bolton, A. J. Coates, F. J. Crary, R. Goldstein, M. Grande, T. W. Hill, R. E. Johnson, R. A. Baragiola, V. Kelha, D. J. McComas, K. Mursula, E. C. Sittler, K. R. Svenes, K. Szego, P. Tanskanen, M. F. Thomsen, S. Bakshi, B. L. Barraclough, Z. Bebesi, D. Delapp, M. W. Dunlop, J. T. Gosling, J. D. Furman, L. K. Gilbert, D. Glenn, C. Holmlund, J.-M. Illiano, G. R. Lewis, D. R. Linder, S. Maurice, H. J. McAndrews, B. T. Narheim, E. Pallier, D. Reisenfeld, A. M. Rymer, H. T. Smith, R. L. Tokar, J. Vilppola and C. Zinsmeyer, Composition and dynamics of plasma in Saturn's magnetosphere, *Science,* **307,** 1262–1266, 2005.